The Eurasia Proceedings of Science, Technology, Engineering & Mathematics (EPSTEM)
ISSN: 2602-3199

The Eurasia Proceedings of Science, Technology, Engineering and Mathematics (EPSTEM), 2025

Volume 36, Pages 93-101

ICBAST 2025: International Conference on Basic Sciences and Technology

Inhomogeneous Planar Structure Experiencing Rotary Motion: A Longitudinal Fracture Investigation

Victor Rizov
University of Architecture, Civil Engineering and Geodesy

Abstract: In different sectors of engineering various planar structures often are experiencing motion. If the motion is with acceleration the inertia loadings in most of the cases cannot be neglected when analyzing different aspects of the behavior (including fracture) of these structures. In modern engineering using of continuously inhomogeneous structural materials for making of different structural members and components is growing constantly. This is due to the excellent properties of these materials. In a result of this, the continuously inhomogeneous materials represent a very promising alternative to the homogeneous engineering materials especially in applications where the structures are subjected to extreme loadings and influences. This paper is focused on investigation of a planar inhomogeneous structure with a longitudinal crack. The structure is experiencing a rotary motion. The inertia loadings induced by the acceleration are taken into account when deriving the strain energy release rate. The members of the structure under consideration are made by a continuously inhomogeneous material having non-linear viscoelastic behavior. Obtaining of the components of the inertia loading that acts on the structure is presented in detail. A verification of the proposed approach against the method of the integral *J* is shown. A parametric study developed by applying the solution of the strain energy release rate under inertia loading is reported and discussed.

Keywords: Planar structure, Rotary motion, Inhomogeneous material, Longitudinal fracture

Introduction

It is well known that using of continuously inhomogeneous structural materials in different segments of the modern engineering has intensified in the recent years. One of the most important features of the continuously inhomogeneous structural materials is that their properties are smooth functions of coordinates. In this relation, the functionally graded materials play a very important role (Gandra et al., 2011, Rizov, 2022; El-Galy et al., 2019). They represent continuously inhomogeneous composites with two or more constituents (Mahamood & Akinlabi, 2017). The constituents are mixed-up during manufacturing so as the microstructure changes smoothly in a solid (Gasik, 2010; Radhika et al., 2020; Rizov, 2018). Thus, there is no distinct border between the constituents of these novel materials in contrast to the fiber or particle reinforced composite materials. In this way, the stress concentrations in functionally graded materials are reduced in a high degree. This is one the basic advantages of the continuously inhomogeneous (functionally graded) materials over the conventional dispersal reinforced composites. One important characteristic of the continuously inhomogeneous materials is that their constituents can be distributed in the process of production so as to achieve a desired profile of continuous properties change along a given direction in a solid. This is a prerequisite for fabrication of members of different engineering structures, mechanisms and facilities of highly efficient characteristics aimed for use in heavy conditions including under dynamic loadings.

The growing use of continuously inhomogeneous materials in various applications in which engineering structures are experiencing motion with acceleration requires conducting of different investigations and analyses of their performance under inertia loadings. The safety and reliability of these structures is closely related to

their fracture behavior (Dowling, 2007; Rizov, 2018; Rizov & Altenbach, 2019). Thus, fracture in structures experiencing motion represents an important subject that has to be studied thoroughly.

This paper is focused on longitudinal fracture in a planar structure experiencing rotary motion. The structure is continuously inhomogeneous along the thickness and length. The mechanical behavior of the structure is non-linear viscoelastic. The strain energy release rate (SERR) in the structure under inertia loading is derived. A verification against the method of the integral *J* is carried-out. A parametric study is performed.

Theoretical Model

The planar structure, $D_1D_2D_4$, has two members, D_1D_2 and D_2D_4, as shown in Figure 1.

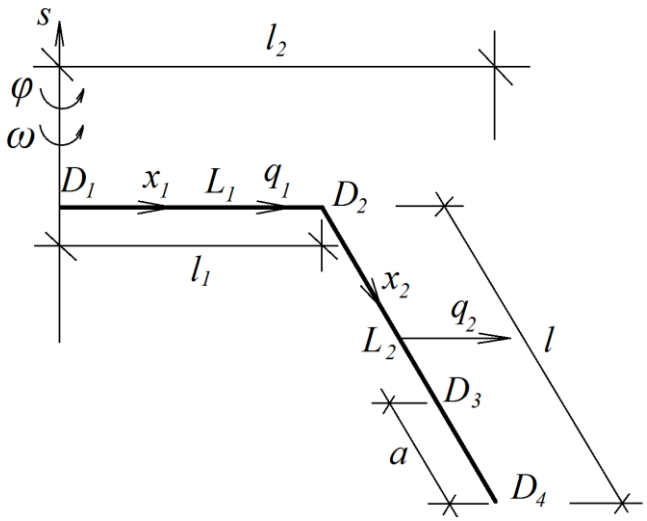

Figure 1. Planar structure, $D_1D_2D_4$, experiencing rotary motion around axis, s

The lengths of these members are l_1 and l, respectively. The thickness of each of the members is h as shown in Figure 2.

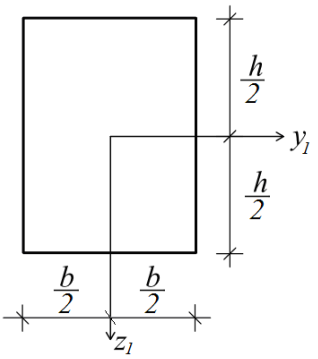

Figure 2. Cross-section of the structure

The members are made by a material that is continuously inhomogeneous along the thickness and length. Thus, the material properties change continuously along h and along the length, $l+l_1$. Besides, the material has non-linear viscoelastic behavior. The structure is experiencing rotary motion around vertical axis, s, according to the law presented in Eq. (1).

$$\varphi = \rho t\,, \tag{1}$$

where φ is the angle of rotation, ρ is a parameter, t is time.

The angular velocity, ω, and acceleration, α, of the planar structure are found by Eqs. (2) and (3), respectively.

$$\omega = \frac{d\varphi}{dt} = \rho\,, \tag{2}$$

$$\alpha = \frac{d\omega}{dt} = 0\,. \tag{3}$$

The normal acceleration, a_{n1}, of an arbitrary point, L_1, of the horizontal structural member, D_1D_2, is found by Eq. (4).

$$a_{n1} = \rho^2 x_1, \tag{4}$$

Where

$$0 \le x_1 \le l_1. \tag{5}$$

The axis, x_1, is shown in Fig. 1 (the origin of x_1 is in point, D_1).

The intensity of the inertia loading, q_1, in point, L_1, is determined by using Eq. (6).

$$q_1 = -a_{n1}m\,, \tag{6}$$

where m is the mass per unit length of the planar structure. The intensity of the inertia loading, q_1, is shown in Figure 1.

Equation (7) is applied for deriving the normal acceleration, a_{n2}, of an arbitrary point, L_2, of the inclined structural member, D_2D_4.

$$a_{n2} = \rho^2\left(l_1 + x_2 \sin\beta\right), \tag{7}$$

Where

$$0 \le x_2 \le l\,, \tag{8}$$

$$\sin\beta = \frac{l_2 - l_1}{l}\,. \tag{9}$$

The axis, x_2, and the size, l_2, are shown in Fig. 1 (the origin of x_2 is in point, D_2).

Equation (10) is used to determine the intensity of the inertia loading, q_2, in point, L_2.

$$q_2 = -a_{n2}m\,. \tag{10}$$

The intensity, q_2, is shown in Figure 1. The relation between stress, σ, strain, ε, and time given in Eq. (11) is applied for modeling the non-linear viscoelastic behavior of the planar structural member (Lukash, 1997).

$$\sigma = B\varepsilon^{\delta}\,\frac{1}{1+\lambda t^{\mu}}\,, \tag{11}$$

where B, δ, λ and μ, are material properties. The changes of these properties along h are presented by the laws given in Eqs. (12), (13), (14) and (15).

$$B = B_1 + \frac{B_2 - B_1}{h^{\psi_B}}\left(\frac{h}{2} + z_1\right)^{\psi_B}, \tag{12}$$

$$\delta = \delta_1 + \frac{\delta_2 - \delta_1}{h^{\psi_\delta}}\left(\frac{h}{2} + z_1\right)^{\psi_\delta}, \tag{13}$$

$$\lambda = \lambda_1 + \frac{\lambda_2 - \lambda_1}{h^{\psi_\lambda}}\left(\frac{h}{2} + z_1\right)^{\psi_\lambda}, \tag{14}$$

$$\mu = \mu_1 + \frac{\mu_2 - \mu_1}{h^{\psi_\mu}}\left(\frac{h}{2} + z_1\right)^{\psi_\mu}, \tag{15}$$

where

$$-\frac{h}{2} \le z_1 \le \frac{h}{2}. \tag{16}$$

In Eqs. (12) – (15), the subscripts, *1* and *2*, refer to the outer and inner surface of the structural members, z_1 is the transversal centric axis of the cross-section (Fig. 2), ψ_B, ψ_δ, ψ_λ and ψ_μ are parameters.

Equations (17) - (24) describe change of material properties along the length of the two members.

$$B_1 = B_{1D1} + \frac{B_{1D4} - B_{1D1}}{(l_1 + l_2)^{\gamma_{B1}}} x_3^{\gamma_{B1}}, \tag{17}$$

$$B_2 = B_{2D1} + \frac{B_{2D4} - B_{2D1}}{(l_1 + l_2)^{\gamma_{B2}}} x_3^{\gamma_{B2}}, \tag{18}$$

$$\delta_1 = \delta_{1D1} + \frac{\delta_{1D4} - \delta_{1D1}}{(l_1 + l_2)^{\gamma_{\delta1}}} x_3^{\gamma_{\delta1}}, \tag{19}$$

$$\delta_2 = \delta_{2D1} + \frac{\delta_{2D4} - \delta_{2D1}}{(l_1 + l_2)^{\gamma_{\delta2}}} x_3^{\gamma_{\delta2}}, \tag{20}$$

$$\lambda_1 = \lambda_{1D1} + \frac{\lambda_{1D4} - \lambda_{1D1}}{(l_1 + l_2)^{\gamma_{\lambda1}}} x_3^{\gamma_{\lambda1}}, \tag{21}$$

$$\lambda_2 = \lambda_{2D1} + \frac{\lambda_{2D4} - \lambda_{2D1}}{(l_1 + l_2)^{\gamma_{\lambda2}}} x_3^{\gamma_{\lambda2}}, \tag{22}$$

$$\mu_1 = \mu_{1D1} + \frac{\mu_{1D4} - \mu_{1D1}}{(l_1 + l_2)^{\gamma_{\mu1}}} x_3^{\gamma_{\mu1}}, \tag{23}$$

$$\mu_2 = \mu_{2D1} + \frac{\mu_{2D4} - \mu_{2D1}}{(l_1 + l_2)^{\gamma_{\mu2}}} x_3^{\gamma_{\mu2}}, \tag{24}$$

where

$$0 \le x_3 \le l_1 + l. \tag{25}$$

In Eqs. (17) – (24), the subscripts, $D1$ and $D4$, refer to sections, $D1$ and $D4$, of the plane structure, x_3 is the longitudinal centric axis, γ_{B1}, γ_{B2}, $\gamma_{\delta1}$, $\gamma_{\delta2}$, $\gamma_{\lambda1}$, $\gamma_{\lambda2}$, $\gamma_{\mu1}$ and $\gamma_{\mu2}$ are parameters.

The SERR, G, is determined by using Eq. (26).

$$G = \frac{dU^*}{bda}, \tag{26}$$

where U^* is the complementary strain energy in the planar structure, da is an elementary increase of the crack length.

The complementary strain energy is found by Eq. (27).

$$U^* = \iiint_{(V)} u_0^* dV, \tag{27}$$

where V is the volume of the structure, u_0^* is the complementary strain energy density.

Equation (28) is applied for determining of u_0^* in an arbitrary point of the structure.

$$u_0^* = \sigma\varepsilon - \int \sigma d\varepsilon, \tag{28}$$

where σ is related to strain, ε, via Eq. (11).

The strain changes along h by the law in Eq. (29).

$$\varepsilon = \kappa\left(z_1 - z_{1n}\right), \tag{29}$$

where

$$-\frac{h}{2} \le z_1 \le \frac{h}{2}. \tag{30}$$

In Eq. (29), κ is the curvature, z_{1n}, is the coordinate of the neutral axis.

The curvature and the coordinate of the neutral axis are determined by applying Eqs. (31) and (32).

$$N = \iint_{(A)} \sigma dA, \tag{31}$$

$$M = \iint_{(A)} \sigma z_1 dA, \tag{32}$$

where N and M are the axial force and the bending moment in the considered section of the structure, A is the area of the section.The axial force and the bending moment are obtained by performing reduction of the inertia loading for the considered section.

A verification of the SERR against the method of the integral *J* is carried-out (Broek, 1986). The integral *J* is obtained by Eq. (33).

$$J = J_1 + J_2 + J_3, \tag{33}$$

where J_1 and J_2 are solutions of the integral *J* in the sections of the inner and outer arms of the crack, J_3 is the solution in the section ahead of the crack tip. Equations (34), (35) and (36) are used for J_1, J_2 and J_3, respectively.

$$J_1=\int\left[u_{01}\cos\alpha_1-\left(p_{x1}\frac{\partial u_1}{\partial x}+p_{y1}\frac{\partial v_1}{\partial x}\right)\right]ds\,, \tag{34}$$

$$J_2=\int\left[u_{02}\cos\alpha_2-\left(p_{x2}\frac{\partial u_2}{\partial x}+p_{y2}\frac{\partial v_2}{\partial x}\right)\right]ds\,, \tag{35}$$

$$J_3=\int\left[u_{03}\cos\alpha_3-\left(p_{x3}\frac{\partial u_3}{\partial x}+p_{y3}\frac{\partial v_3}{\partial x}\right)\right]ds\,. \tag{36}$$

The integration is performed by the MatLab. The solution of the *J* matches the solution of the SERR which is a verification of the present analysis.

Parametric Study

A parametric study is developed with purpose to examine the peculiarities of the longitudinal fracture in a continuously inhomogeneous planar structure experiencing rotary motion. In particular, we are focused on the parameters of the motion law, the geometry of the structure, and the material inhomogeneity. The study clarifies the influence of these parameters on the SERR. The results of the parametric study are reported graphically in Figs. 3, 4, 5 and 6. The SERR is obtained for $b=0.010$ m, $h=0.015$ m, $a=0.5l$, $\psi_B=0.4$, $\psi_\delta=0.4$, $\psi_\lambda=0.4$, $\psi_\mu=0.4$, $\gamma_{B1}=0.6$, $\gamma_{B2}=0.6$, $\gamma_{\delta1}=0.6$, $\gamma_{\delta2}=0.6$, $\gamma_{\lambda1}=0.8$, $\gamma_{\lambda2}=0.8$, $\gamma_{\mu1}=0.8$ and $\gamma_{\mu2}=0.8$.

First, the effects of the parameter, ρ, of the rotary motion on the SERR are examined at $B_{1D4}/B_{1D1}=0.5$ (curve 1), $B_{1D4}/B_{1D1}=1.0$ (curve 2), and $B_{1D4}/B_{1D1}=2.0$ (curve 3) in Figure 3. The growth of the SERR that can be seen in Figure 3 with increase of the value of ρ is generated by increase of the inertia loading. Increase of B_{1D4}/B_{1D1} ratio reduces the SERR (Figure 3).

One can observe how the SERR is influenced by B_{2D4}/B_{2D1} ratio at $l/h=10$ (curve 1), $l/h=15$ (curve 2), and $l/h=20$ (curve 3) in Figure 4.

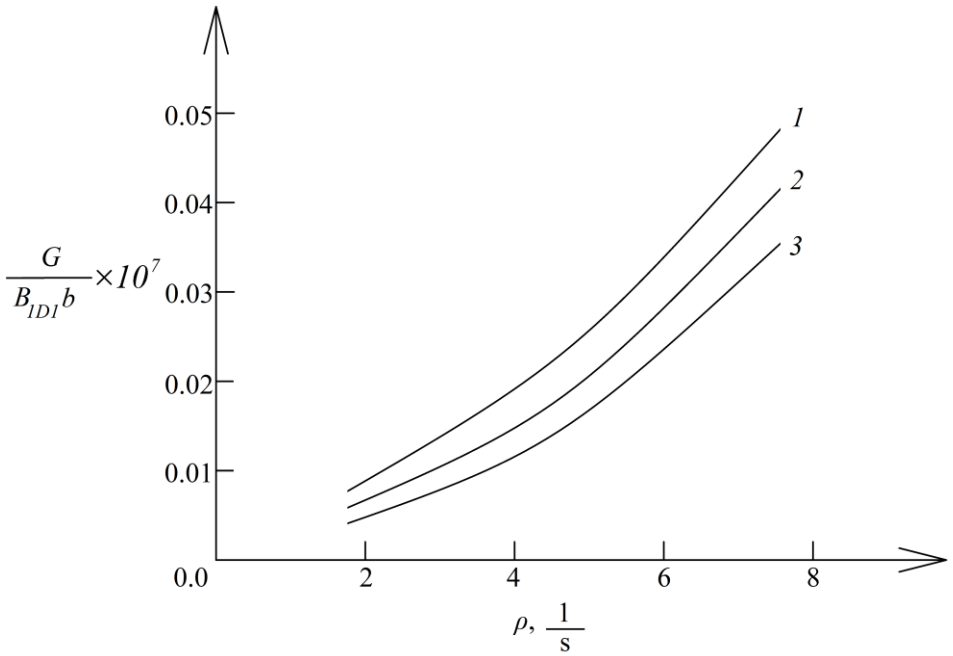

Figure 3. The SERR versus ρ

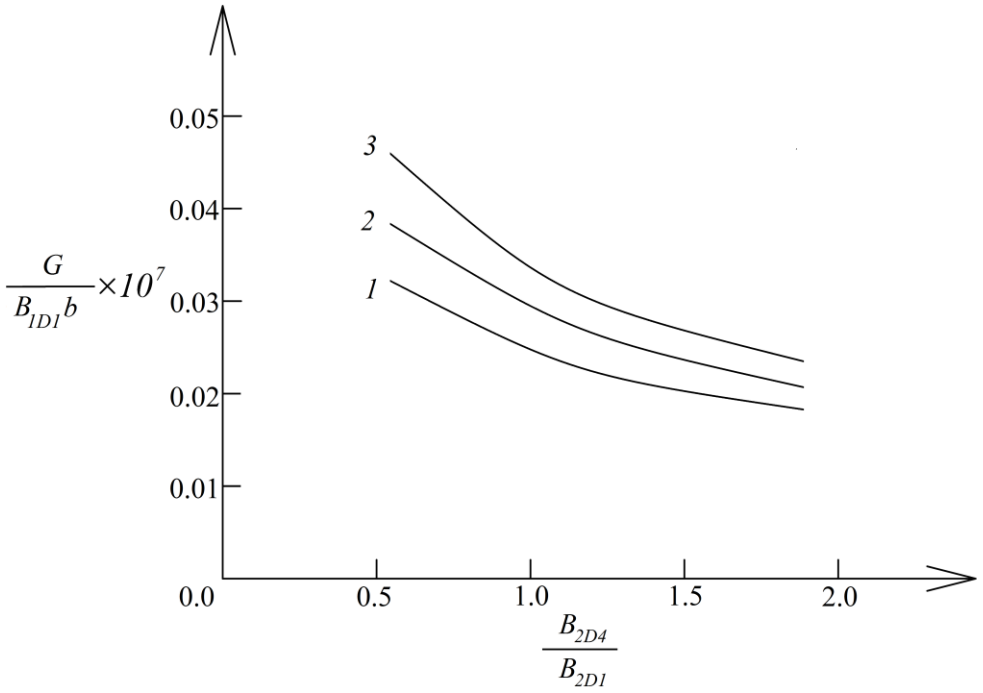

Figure 4. The SERR versus B_{2D4}/B_{2D1} ratio

The rise of the SERR with increase of l/h ratio that can be observed in Figure 4 is induced again by the growth of the inertia loading. The SERR reduces as a result of the growth of B_{2D4}/B_{2D1} ratio (Figure 4).

Figure 5 gives an idea about the effects of l_1/h ratio on the SERR at $\delta_{1D4}/\delta_{1D1}=0.5$ (curve 1), $\delta_{1D4}/\delta_{1D1}=1.0$ (curve 2), and $\delta_{1D4}/\delta_{1D1}=2.0$ (curve 3). Rise of l_1/h ratio generates a growth of the SERR (Figure 5). This is due to increase of the inertia loading induced by the rise the length, l_1. Increase of $\delta_{1D4}/\delta_{1D1}$ ratio reduces the SERR as one can see in Figure 5.

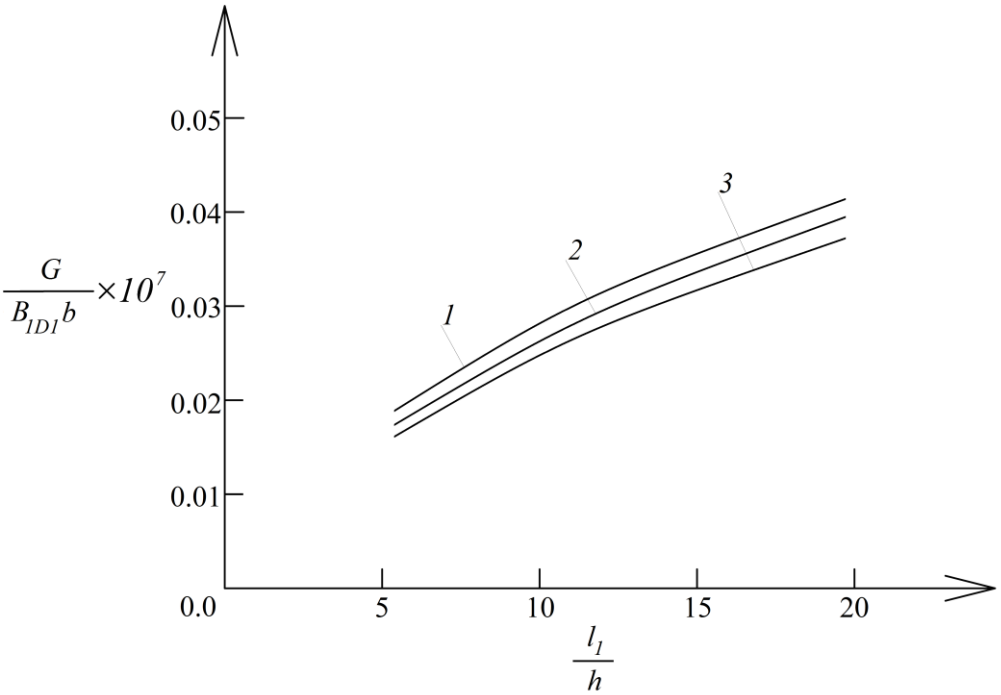

Figure 5. The SERR versus l_1/h ratio

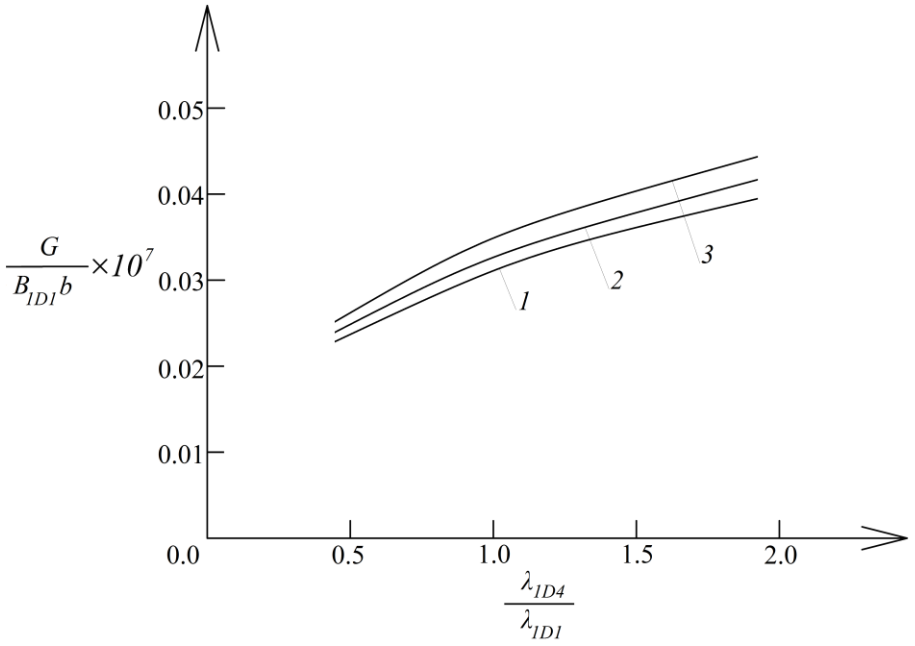

Figure 6. The SERR versus $\lambda_{1D4}/\lambda_{1D1}$ ratio

Finally, we examine how the SERR is influenced by $\lambda_{1D4}/\lambda_{1D1}$ ratio at $l_2/h=4$ (curve 1), $l_2/h=8$ (curve 2), and $l_2/h=12$ (curve 3) in Figure 6. The examination reveals that the SERR grows as a result of increase of $\lambda_{1D4}/\lambda_{1D1}$ ratio as one can observe in Figure 6. Increase of l_2/h ratio leads to also to growth of the SERR as shown in Figure 6.

Conclusion

In conclusion, it can be stated that the investigation developed in this paper throws light on the peculiarities of longitudinal fracture in continuously inhomogeneous non-linear viscoelastic planar structures experiencing rotary motion. The solution of the SERR under inertia loading derived here is used for performing a parametric study. It is found that the SERR is strongly affected by the law of rotary motion, the geometry of the planar structure and the inhomogeneity of the material. The increase of parameter, ρ, of the rotary motion induces a growth of the SERR. Increase of l/h, l_1/h and l_2/h ratios (these ratios represent geometrical parameters of the planar structure) induces also a growth of the SERR. Opposite trend, i.e. reduction of the SERR is detected when B_{1D4}/B_{1D1}, B_{2D4}/B_{2D1} and $\delta_{1D4}/\delta_{1D1}$ ratios increase.

Recommendations

The results obtained in this paper indicate that the approach can be used for analyzing longitudinal fracture in rotating planar structures. The approach can be applied also for rotating structures of more complex geometry.

Scientific Ethics Declaration

*The author declares that the scientific ethical and legal responsibility of this article published in EPSTEM journal belongs to the author.

Funding

* This research received no specific grant from any funding agency in the public, commercial, or not-for-profit sectors.

Conflict of Interest

*The author declares that he has no conflicts of interest.

Acknowledgements or Notes

*This article was presented as an oral presentation at the International Conference on Basic Sciences and Technology (www.icbast.net) held in Budapest/Hungary on August 28-31, 2025.

References

Broek, D. (1986). *Elementary engineering fracture mechanics*. Springer.

Dowling, N. (2007). *Mechanical behavior of materials*. Pearson.

El-Galy, I.M., Saleh, B.I., & Ahmed, M.H. (2019). Functionally graded materials classifications and development trends from industrial point of view. *SN Applied Sciences, 1,* 1378.

Gandra, J., Miranda, R., Vilaça, P., Velhinho, A., & Teixeira, J.P. (2011). Functionally graded materials produced by friction stir processing. *Journal of Materials Processing Technology*, *211,* 1659-1668.

Gasik, M. M. (2010). Functionally graded materials: bulk processing techniques. *International Journal of Materials and Product Technology*, *39*, 20-29.

Lukash, P. (1997). *Fundamentals of non-linear structural mechanics*. Science.

Mahamood, R. C., & Akinlabi, E. T. (2017). *Functionally graded materials.* Springer.

Radhika, N., Sasikumar, J., Sylesh, J. L., & Kishore, R. (2020). Dry reciprocating wear and frictional behaviour of B4C reinforced functionally graded and homogenous aluminium matrix composites. *Journal of Materials Research and Technology*, *9,* 1578-1592.

Rizov, V. I. (2018). Non-linear delamination in two-dimensional functionally graded multilayered beam. *International Journal of Structural Integrity, 9,* 646-663.

Rizov, V. I. (2022). Effects of periodic loading on longitudinal fracture in viscoelastic functionally graded beam structures. *Journal of Applied and Computational Mechanics, 8,* 370–378.

Rizov, V.I., & Altenbach, H. (2019). On the analysis of lengthwise fracture of functionally graded round bars. *Structural Integrity and Life*, *19*, 102–108.

Author(s) Information

Victor Rizov
University of Architecture, Civil Engineering and Geodesy
1 Chr. Smirnensky blvd., 1046 – Sofia, Bulgaria
Contact e-mail: *v_rizov_fhe@uacg.bg*

To cite this article:

Rizov, V. (2025). Inhomogeneous planar structure experiencing rotary motion: A longitudinal fracture investigation. *The Eurasia Proceedings of Science, Technology, Engineering and Mathematics (EPSTEM), 36,* 93-101.